Heterostructures based on inorganic and organic van der Waals systems

Gwan-Hyoung Lee, Chul-Ho Lee, Arend M. van der Zande, Minyong Han, Xu Cui, Ghidewon Arefe, Colin Nuckolls, Tony F. Heinz, James Hone, and Philip Kim

Citation: APL Materials **2**, 092511 (2014); doi: 10.1063/1.4894435
View online: http://dx.doi.org/10.1063/1.4894435
View Table of Contents: http://scitation.aip.org/content/aip/journal/aplmater/2/9?ver=pdfcov
Published by the AIP Publishing

Heterostructures based on inorganic and organic van der Waals systems

Gwan-Hyoung Lee,[1,a] Chul-Ho Lee,[2,a] Arend M. van der Zande,[3] Minyong Han,[4] Xu Cui,[5] Ghidewon Arefe,[5] Colin Nuckolls,[6] Tony F. Heinz,[7,8] James Hone,[5] and Philip Kim[4,8,b]

[1]*Department of Materials Science and Engineering, Yonsei University, Seoul 120-749, South Korea*
[2]*KU-KIST Graduate School of Converging Science and Technology, Korea University, Seoul 136-701, South Korea*
[3]*Energy Frontier Research Center (EFRC), Columbia University, New York, New York 10027, USA*
[4]*Department of Applied Physics and Applied Mathematics, Columbia University, New York, New York 10027, USA*
[5]*Department of Mechanical Engineering, Columbia University, New York, New York 10027, USA*
[6]*Department of Chemistry, Columbia University, New York, New York 10027, USA*
[7]*Department of Electrical Engineering, Columbia University, New York, New York 10027, USA*
[8]*Department of Physics, Columbia University, New York, New York 10027, USA*

(Received 28 July 2014; accepted 21 August 2014; published online 2 September 2014)

The two-dimensional limit of layered materials has recently been realized through the use of van der Waals (vdW) heterostructures composed of weakly interacting layers. In this paper, we describe two different classes of vdW heterostructures: inorganic vdW heterostructures prepared by co-lamination and restacking; and organic-inorganic hetero-epitaxy created by physical vapor deposition of organic molecule crystals on an inorganic vdW substrate. Both types of heterostructures exhibit atomically clean vdW interfaces. Employing such vdW heterostructures, we have demonstrated various novel devices, including graphene/hexagonal boron nitride (hBN) and MoS_2 heterostructures for memory devices; graphene/MoS_2/WSe_2/graphene vertical *p-n* junctions for photovoltaic devices, and organic crystals on hBN with graphene electrodes for high-performance transistors. [http://dx.doi.org/10.1063/1.4894435]

Since the isolation of graphene a decade ago, many van der Waals (vdW) materials, including insulators, semiconductors, metals, superconductors, and topological insulators, have been produced as two-dimensional (2D) sheets with thicknesses down to the limit of a single layer.[1,2] Recently, there have been important advances in the technology to controllably stack 2D vdW materials to create functional interfaces between dissimilar vdW materials.[3,4] Using these techniques, we can now form heterostructures from a wide variety of starting materials, with a controllable number of atomic layers and atomically sharp interfaces.

The ability to combine materials with diverse properties into layered heterostructures lies at the heart of modern electronics and can lead to new material properties and emergent behavior at interfaces.[5] In conventional materials, lattice matching and other considerations limit the materials that can be combined, and the quality of interfaces that can be achieved. This limitation can be circumvented by the use of 2D vdW materials discussed above, which have weak out-of-plane bonding. Inspired by the great success of graphene research, an interest has developed in a new

[a]G.-H. Lee and C.-H. Lee contributed equally to this work.
[b]E-mail: pk2015@columbia.edu

class of available 2D systems. These atomically thin layered materials can be isolated from strongly anisotropic bulk materials, such as hexagonal boron nitride (hBN), transition metal dichalcogenides (TMDCs), and organic materials, where weak vdW forces hold the layers together. Unlike conventional semiconductor heterostructures, these vdW layered materials consist of in-plane covalently bonded atomic layers that interact only weakly with other constituents in the out-of-plane direction. This weak interlayer interaction allows in principle the stacking of a wide range of 2D vdW materials together without the requirement of atomic scale commensurability. Therefore, the combination of different layered constituents may produce heterogeneous and functional materials whose interfaces yield completely different types of 2D electronic systems. These systems can demonstrate unique physical properties, providing the opportunity to build novel quantum electronic devices based on emergent collective phenomena.[6–8]

In this paper, we describe recent developments in the creation of novel heterostructures based on both inorganic and organic vdW systems. Two different approaches will be discussed: (i) the co-lamination and restacking of vdW heterostructures; and (ii) physical vapor deposition on a vdW substrate. The first method is based on an extension of mechanical exfoliation techniques and co-lamination to controllably stack various inorganic 2D vdW materials. This enables the construction of atomically engineered heterostructures from a wide range of inorganic vdW materials. Furthermore, new techniques provide electrical contacts to fully encapsulated active layers.[4] The second technique utilizes vdW surfaces as a template for epitaxial growth of highly ordered, crystalline organic and inorganic films. 2D materials such as graphene, hBN, and semiconducting TMDCs offer a new type of substrate for the growth of high-quality semiconductor films via vdW heteroepitaxy. The absence of dangling bonds and charge traps on the surface of vdW substrates enables the formation of the atomically well-defined interfaces with the depositing materials by physical vapor deposition. The concomitant reduction in the density of the charge traps and/or scattering centers can greatly improve the transport properties of the deposited layer and the associated device operation.

The structure of paper is as follows. We first discuss the two different approaches to create vdW heterostructures described above. We then present three different examples of vdW heterostructures and their characteristics: (i) MoS_2/hBN/graphene heterostructures for memory devices; (ii) multilayer graphene/MoS_2/WSe_2/graphene vertical *p-n* junction devices; and (iii) high-performance rubrene devices prepared on hBN with graphene electrodes. Parts of these studies have been previously reported, where additional details may be found.[9–11]

We construct the functional heterostructures of inorganic vdW materials simply by stacking atomically thin layers on top of one another by successive transfer steps (see Fig. 1(a)). In order to transfer one 2D layer onto another, a thin polymer film has previously been utilized, as reported by Dean *et al.*[3] This technique enables multiple-stacking of 2D materials and fabrication of high performance graphene devices on hBN.[3,12] However, the formation of bubbles and the presence of organic residues at the interfaces have typically been observed in the process due to the use of a polymer film, even after cleaning and high-temperature annealing between stacking steps. This leads to degradation of the performance of 2D layers and to difficulties in large-area device fabrication.[4,12] We have therefore developed two different polymer-free transfer techniques for the assembly of clean, atomically-sharp vdW interfaces.[4,13]

The first method for polymer-free assembly, the polydimethylsiloxane (PDMS) transfer technique shown in Fig. 1(b), uses a PDMS elastomer stamp instead of a polymer layer to support the 2D sheet.[13] 2D materials are exfoliated directly onto the PDMS stamp and can then be transferred onto a target 2D material on an arbitrary substrate, whether rigid or flexible. The second method, the pick-up transfer technique shown in Fig. 1(c), employs a sheet of hBN to pick up a 2D layer of the material of interest using the mutual vdW interaction between the layers.[4] In detail, a flake of hBN is mechanically exfoliated onto a bare Si chip coated with a thin poly-propylene carbonate (PPC) film. The PPC film then carefully peeled off the substrate and placed onto a PDMS stamp. The hBN flake placed in contact with the target 2D layer, which was separately prepared on a SiO_2/Si substrate. After heating to 40 °C, the PDMS stamp is gently lifted up to pick up the whole stack. This process is repeated to produce the desired multiple-stack. The entire stack is finally transferred onto the chosen substrate by melting the PPC film at 90 °C to remove the PDMS stamp, and dissolving the PPC in chloroform.

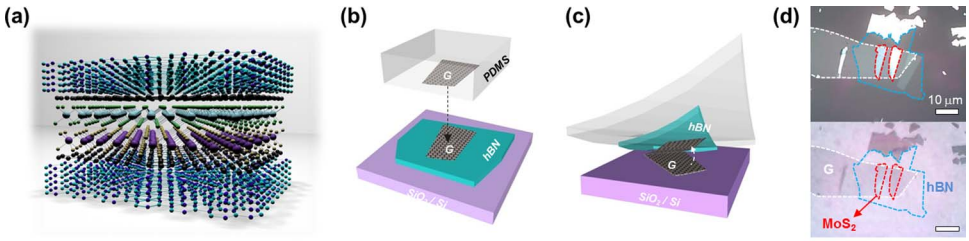

FIG. 1. (a) Schematic illustration of vdW a heterostructure consisting of a multiple-stack of hBN/graphene/MoS_2/WSe_2/graphene/hBN. The stacking techniques of (b) PDMS transfer and (c) pick-up transfer show how a graphene flake is transferred onto an hBN flake. (d) Optical images in reflection (upper) and transmission (lower) of a stack of MoS_2 (3 layers)/hBN (10 nm)/graphene (5 layers).

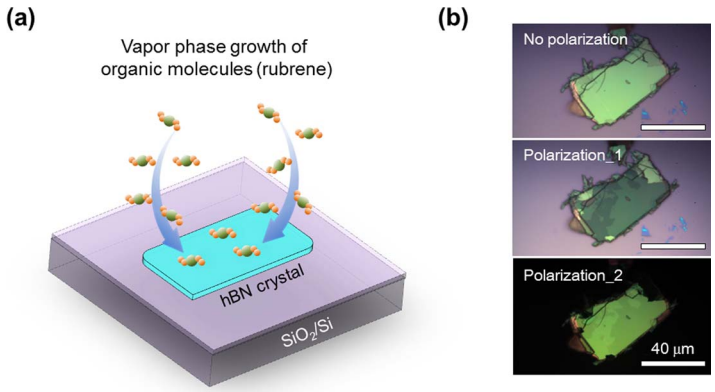

FIG. 2. (a) Schematic illustration of vapor phase growth of organic molecules on the hBN crystal. (b) Non-polarized and polarized optical images of the rubrene film grown on hBN.

By employing these techniques, ultraclean and atomically-sharp vdW heterointerfaces of inorganic/inorganic and organic/inorganic materials can be fabricated.[13,14] The advantage of these methods is confirmed by the superior performance of graphene devices produced by these techniques compared with those prepared by methods utilizing a polymer film.[4,13,14] Figure 1(d) shows a representative stack of MoS_2 (3 layers)/hBN (10 nm)/graphene (5 layers) on a PDMS stamp created by these techniques. The transmission-mode optical image of Fig. 1(d) shows that this stack is highly transparent and bubble-free. For device fabrication, the stacks can be shaped to the desired device structure through e-beam patterning and reactive ion etching (RIE). Electrodes can then be patterned by e-beam lithography and subsequent metal deposition. When an active 2D material is encapsulated between two hBN flakes, the encapsulated 2D material can be fully protected during the entire device fabrication process. This approach avoids polymer resists and solutions that can influence the characteristics of 2D materials, as well as environmental conditions, such as reactive chemical species and water molecules that can also affect the electrical and optical properties of 2D sheets.[15,16]

In addition to vdW hetero-assembly described above, epitaxial growth provides an alternative route to fabricate heterostructures based on numerous vdW systems. In particular, organic materials can also create vdW heterostructures by interfacing with 2D inorganic materials such as graphene, hBN, and TMDCs to form high quality atomically sharp interfaces with vdW interactions. We have already demonstrated epitaxial growth of an organic film on 2D layered materials such as hBN and graphene.[10] Figure 2(a) shows a schematic illustration of vapor-phase growth of rubrene on hBN crystallites mechanically exfoliated on SiO_2/Si substrates. A purified source of rubrene powder was sublimated in a hot zone at 230 °C. The vaporized molecules were transported to the crystalline zone at 180 °C by flowing Ar carrier gas under vacuum (~1 Torr), where the substrate was placed for

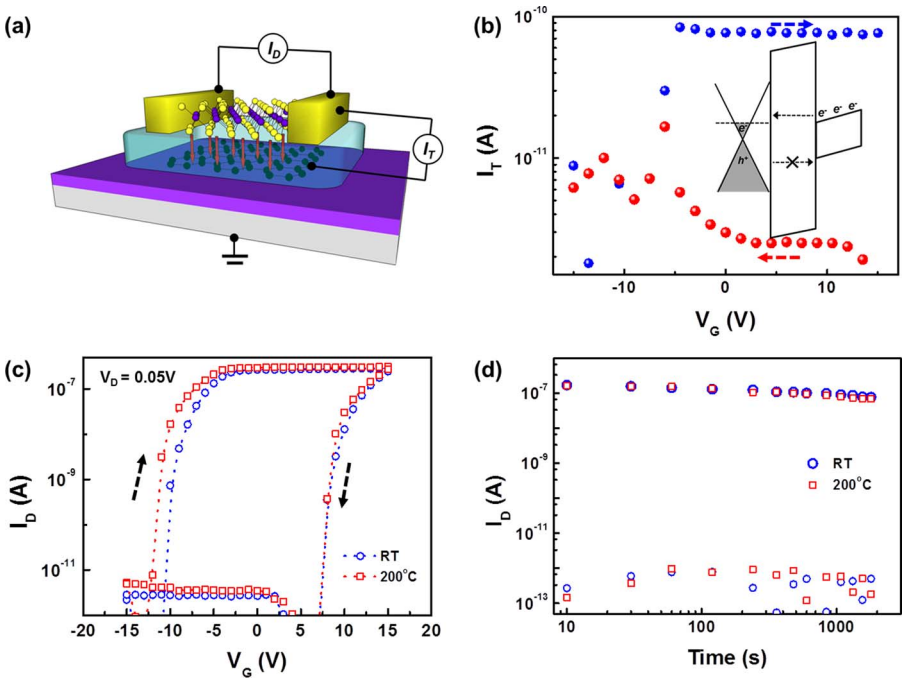

FIG. 3. (a) Schematic of vdW heterostructure memory device consisting of MoS_2/hBN/graphene. (b) Tunneling current (I_T) between MoS_2 and graphene through hBN with varying gate voltage (V_G) of forward and backward sweep directions. The inset shows the band alignment of heterostructure and tunneling of electrons. (c) Transfer curve of drain current (I_D) shows a large hysteresis at room temperature and 200 °C. (d) Retention curve shows high on/off ratio and nonvolatile characteristics of the heterostructure memory device at room temperature and 200 °C. The retention was measured at $V_G = 0$ V with pulse of ±15 V, pulse width of 100 μs, and $V_D = 50$ mV.

the organic crystal growth. To avoid unintentional contamination of the hBN surface, the substrate was cleaned via vacuum annealing at 400 °C prior to the growth. We mainly controlled the substrate temperature for optimization of the crystal growth, and obtained the highest crystal quality at 180 ± 10 °C. The amorphous films were grown on the entire substrate without surface selectivity at lower temperatures, while no growth occurs on the surface at higher temperatures. Under optimal conditions, we could grow high-quality rubrene crystalline films with large domains selectively on the hBN surface. This large domain growth of a crystalline film was characterized with polarized optical microscopy since crystallographic anisotropy of the rubrene crystal could result in the optical contrast in the polarized images depending on in-plane orientations as shown in Fig. 2(b). It should be noted that optimal growth conditions can differ depending on other growth parameters as well as organic molecules.

vdW heterostructures formed by stacking 2D materials have a great potential for next-generation electronics because of the outstanding properties of the constituent materials. In particular, their high uniformity and ability to tune the number of layers is promising for memory devices based on charge tunneling. For example, graphene and graphene oxide have been used for memory devices,[17,18] while more advanced memory devices based on the vdW heterostructure was recently demonstrated.[9] Nonvolatile heterostructured memory devices of Fig. 3(a) were fabricated on a Si wafer with 280 nm-thick SiO_2 by stacking 2D materials, which consist of MoS_2 (channel), hBN (tunneling barrier), and graphene (charge trapping layer). Electrodes were formed by electron beam lithography and deposition of Au (50 nm) and the doped Si substrate was used as a back gate. As shown in Fig. 3(a), the drain current of MoS_2 (I_D) and tunneling current (I_T) between MoS_2 and graphene through hBN were measured to verify the memory performance and tunneling mechanism. According to the band alignment of the inset of Fig. 3(b), it can be inferred that both electrons and holes can tunnel through the hBN barrier in the MoS_2/hBN/graphene heterostructure. However, hole tunneling through hBN layer is less feasible due to relatively larger effective mass and higher barrier height for

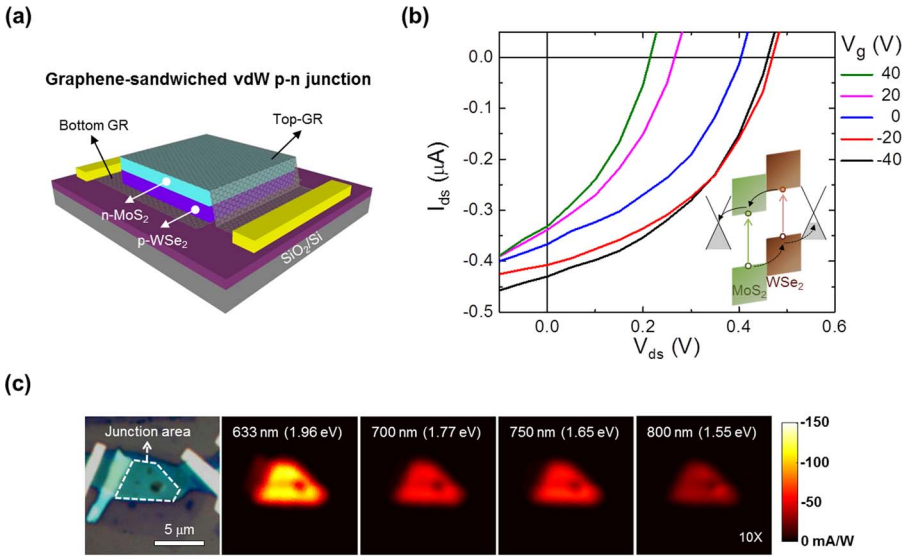

FIG. 4. (a) Schematic of graphene-sandwiched multilayer p-WSe_2/n-MoS_2 heterostructure. (b) Photovoltaic characteristics of the p-n junction at various gate voltages. The curves were measured using a focused 532-nm laser with a power of ~3.7 μW. The inset shows the band diagram of the junction. The band slopes and potential barriers (mainly between graphene and WSe_2) would be changed as the gate voltage varies. (c) Photocurrent maps (at $V_{ds} = 0$ V) with the focused laser excitation with different wavelengths. An optical micrograph of the device is shown in the left. The thicknesses of WSe_2 and MoS_2 layers are 9 nm and 10 nm, respectively.

holes.[9,19] When I_T was measured as shown in Fig. 3(b), it was observed that electrons in MoS_2 are transferred by tunneling through hBN and trapped in floating graphene when the gate voltage (V_G) is positive in a trapping process (forward sweep of V_G); meanwhile the trapped electrons tunnel back to MoS_2 when V_G is negative in a releasing process (backward sweep). As a result, the trapped electrons in the graphene layer, which acts as a floating gate,[20] give rise to a large hysteresis of MoS_2 transfer curve. As shown in Fig. 3(c), the transfer curve of the MoS_2/hBN/graphene heterostructure device exhibited a large hysteresis of $\Delta V \approx 20$ V and high on/off current ratio of $\sim 10^5$. Furthermore, even at high temperature of 200 °C, no appreciable difference was observed in device operation, confirming the high stability of vdW heterostructure. As expected from this, the heterostructure memory devices show good retention and endurance characteristics.[9] As shown in Fig. 3(d), we also verified that high on/off ratio can be maintained for a long time of over 1000 s at room temperature and even at 200 °C. Therefore, we can conclude that the vdW heterostructure memory devices are a promising candidate for nonvolatile memory applications, which require high transparency, flexibility, and operational stability in harsh conditions.

In addition to the electronic applications, vdW heterostructures based on 2D semiconductors with controllable band gaps and doping can be exploited for optoelectronic devices such as photodiodes, solar cells, and light-emitting diodes.[11,21–24] The most fundamental unit is a p-n junction, which can be realized by vertically stacking the TMDC layers with different doping. Figure 4(a) represents a schematic of the graphene-sandwiched multilayer p-WSe_2/n-MoS_2 junction device. We used the "pick-up transfer" technique described above. A multi-stacked vdW heterostructure was constructed by conducting multiple pick-up processes sequentially. In this device geometry, we employed graphene layers as charge-collecting contacts, which are separately connected to metal electrodes by the edge-contact scheme.[4]

The vdW p-n junction exhibited the rectifying diode behavior and photovoltaic response as reported previously.[11] More interestingly, the device characteristics of a p-n junction can be tuned by varying the gate voltage. Figure 4(b) shows current-voltage (I–V) curves under 532-nm laser illumination at various gate voltages. The characteristics clearly demonstrate gate-tunable photovoltaic operation. Upon sweeping the gate voltage to the negative direction, the open-circuit voltage and the short-circuit current tend to increase, reaching maxima of 0.47 V and 116 mA/W, respectively. This

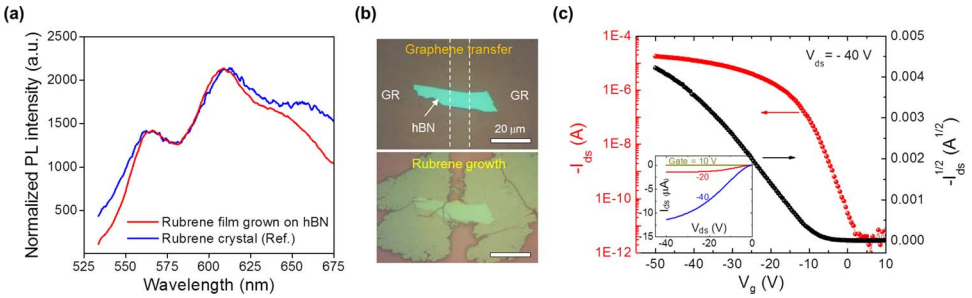

FIG. 5. (a) Representative PL spectra of the rubrene film grown on hBN and free-standing rubrene crystal. (b) Optical micrographs of graphene (GR) pads transferred on the hBN crystal (top) and the rubrene film grown on the graphene/hBN/graphene structure. (c) Representative transfer characteristic of the fabricated FET. The inset shows the output characteristic of the device.

trend can be attributed to increase of band slopes in the p-n junction and decrease of the potential barrier between graphene and WSe_2 because the layers close to the back-gate become more p-doped electrostatically as the gate voltage varies in the negative direction. These will enhance charge separation and collection in the p-n junction. Note that the gate-tunable characteristics are possible owing to weak electrostatic screening of ultrathin materials and absence of the Fermi-level pining at the atomically sharp heterointerfaces, offering a unique opportunity to realize tunable optoelectronic devices.

The spatial origin of the observed photovoltaic responses was further investigated by scanning photocurrent measurements. Figure 4(c) shows photocurrent maps with different excitation energies. Regardless of wavelength, we observed uniform photocurrent dominantly from the overlapped junction area, indicating that photovoltaic action is originated from the p-n junction sandwiched between top and bottom graphene layers. In addition, the wavelength-dependent photo-response suggests that both TMDC layers absorb light and contribute to the photocurrent. We believe that further optimization of the band alignment, doping, and cell thickness can enable the realization of efficient photovoltaic cells by multiple vdW assemblies of 2D semiconductors.

We already demonstrated that rubrene can be epitaxially grown on the hBN surface with small misorientation between two crystal lattices, enabling the growth of rubrene films with large single-crystalline domains.[10] In addition to crystal quality, the optical quality of rubrene films grown on hBN is comparable to that of a free-standing rubrene crystal. Figure 5(a) shows comparison of photo luminescence (PL) spectra for two samples prepared differently. The rubrene film grown on hBN showed the main PL peak at ~615 nm and the broad shoulder around 650 nm, similar with those of a free-standing single crystal separately prepared.[25]

High-quality organic crystalline films on dielectric materials are useful for the fabrication of high-performance organic field effect transistors (FETs). In particular, a vdW dielectric such as hBN is more desirable because it forms a very clean channel-dielectric interface. For further realization of a FET geometry, we used graphene as a vdW electrode. As shown in the top of Fig. 5(b), the patterned chemical-vapor-deposited graphene films were transferred on the hBN surface using the "PDMS transfer" technique. Then, rubrene films were grown on the lateral graphene/hBN/graphene heterostructure under same growth conditions. Owing to atomic thinness and vdW nature of graphene, we still grew high-quality rubrene films uniformly across the entire structure as shown in the bottom of Fig. 5(b). Furthermore, reasonably good electrical contact was achieved at room temperature when compared with typical metal contacts as reported previously.[10] The fabricated device exhibited excellent transistor characteristics with high mobility and on/off ratio. The field-effect mobility extracted from Fig. 5(c) was 2.9 cm^2/V s, and average values were 5.1 ± 2.7 cm^2/V s. These values are comparable to those of rubrene single crystal devices fabricated on SiO_2/Si substrates. Although we have demonstrated one specific example, the principle of organic/inorganic vdW heteroepitaxy can be easily generalized where these functioning organic and inorganic vdW heterostructures have a great potential for various electronic and optoelectronic applications.

We have developed the methods creating inorganic/inorganic heterostructures using co-lamination and restacking vdW materials. We also demonstrate organic/inorganic heterostructures by

epitaxial growth of an organic crystal on the surface of vdW materials. Using these functional hetero-interfaces, furthermore, we demonstrate several novel device operations. In MoS_2/hBN/graphene tunneling devices, we build a non-volatile memory device utilizing charge tunneling across the vdW interfaces. We also show vdW p-n junctions by sandwiching the multilayer p-WSe_2/n-MoS_2 heterostructure with graphene electrodes. The junction exhibits both gate-tunable rectifying electrical characteristics and photovoltaic responses. Finally, we demonstrate high-performance organic electronic devices by utilizing rubrene crystalline films grown on hBN with atomically thin graphene electrodes contacting the accumulated charge carriers via the electrical field effect at the vdW interface. Further, optimization and atomic control of these organic/inorganic vdW interfaces will provide novel functional material platforms where one can realize high-performance electronic and optoelectronic devices.

This work was partially supported by the National Science Foundation (DMR-1124894) and by the FAME Center, one of the six centres of STARnet, a Semiconductor Research Corporation program sponsored by MARCO and DARPA. G.H.L. and M.H. acknowledge support from Basic Science Research Program (2014R1A1A1004632) (G.H.L.) and the Nano Material Technology Development Program (2012M3A7B4049966) (M.H.) through the National Research Foundation of Korea (NRF) funded by the Ministry of Science, ICT and Future Planning.

[1] K. S. Novoselov, A. K. Geim, S. V. Morozov, D. Jiang, Y. Zhang, S. V. Dubonos, I. V. Grigorieva, and A. A. Firsov, Science **306**, 666 (2004).
[2] K. S. Novoselov, D. Jiang, F. Schedin, T. J. Booth, V. V. Khotkevich, S. V. Morozov, and A. K. Geim, Proc. Natl. Acad. Sci. U.S.A. **102**, 10451 (2005).
[3] C. R. Dean, A. F. Young, I. Meric, C. Lee, L. Wang, S. Sorgenfrei, K. Watanabe, T. Taniguchi, P. Kim, K. L. Shepard, and J. Hone, Nat. Nanotechnol. **5**, 722 (2010).
[4] L. Wang, I. Meric, P. Y. Huang, Q. Gao, Y. Gao, H. Tran, T. Taniguchi, K. Watanabe, L. M. Campos, D. A. Muller, J. Guo, P. Kim, J. Hone, K. L. Shepard, and C. R. Dean, Science **342**, 614 (2013).
[5] A. K. Geim and I. V. Grigorieva, Nature **499**, 419 (2013).
[6] L. Britnell, R. V. Gorbachev, R. Jalil, B. D. Belle, F. Schedin, A. Mishchenko, T. Georgiou, M. I. Katsnelson, L. Eaves, S. V. Morozov, N. M. R. Peres, J. Leist, A. K. Geim, K. S. Novoselov, and L. A. Ponomarenko, Science **335**, 947 (2012).
[7] C. R. Dean, L. Wang, P. Maher, C. Forsythe, F. Ghahari, Y. Gao, J. Katoch, M. Ishigami, P. Moon, M. Koshino, T. Taniguchi, K. Watanabe, K. L. Shepard, J. Hone, and P. Kim, Nature **497**, 598 (2013).
[8] L. Britnell, R. M. Ribeiro, A. Eckmann, R. Jalil, B. D. Belle, A. Mishchenko, Y. J. Kim, R. V. Gorbachev, T. Georgiou, S. V. Morozov, A. N. Grigorenko, A. K. Geim, C. Casiraghi, A. H. C. Neto, and K. S. Novoselov, Science **340**, 1311 (2013).
[9] M. S. Choi, G. H. Lee, Y. J. Yu, D. Y. Lee, S. H. Lee, P. Kim, J. Hone, and W. J. Yoo, Nat. Commun. **4**, 1624 (2013).
[10] C.-H. Lee, T. Schiros, E. J. G. Santos, B. Kim, K. G. Yager, S. J. Kang, S. Lee, J. Yu, K. Watanabe, T. Taniguchi, J. Hone, E. Kaxiras, C. Nuckolls, and P. Kim, Adv. Mater. **26**, 2812 (2014).
[11] C.-H. Lee, G.-H. Lee, A. M. van der Zande, W. Chen, Y. Li, M. Han, X. Cui, G. Arefe, C. Nuckolls, T. F. Heinz, J. Guo, J. Hone, and P. Kim, "Atomically thin p–n junctions with van der Waals heterointerfaces," Nat. Nanotechnol. (published online).
[12] S. J. Haigh, A. Gholinia, R. Jalil, S. Romani, L. Britnell, D. C. Elias, K. S. Novoselov, L. A. Ponomarenko, A. K. Geim, and R. Gorbachev, Nat. Mater. **11**, 764 (2012).
[13] G.-H. Lee, Y.-J. Yu, X. Cui, N. Petrone, C.-H. Lee, M. S. Choi, D.-Y. Lee, C. Lee, Y. J. Yoo, K. Watanabe, T. Takahashi, C. Nuckolls, P. Kim, and J. Hone, ACS Nano **7**, 7931 (2013).
[14] S. J. Kang, G.-H. Lee, Y.-J. Yu, Y. Zhao, B. Kim, K. Watanabe, T. Taniguchi, J. Hone, P. Kim, and C. Nuckolls, Adv. Funct. Mater. **24**, 5157 (2014).
[15] D. J. Late, B. Liu, H. S. S. R. Matte, V. P. Dravid, and C. N. R. Rao, ACS Nano **6**, 5635 (2012).
[16] S. Tongay, J. Zhou, C. Ataca, J. Liu, J. S. Kang, T. S. Matthews, L. You, J. B. Li, J. C. Grossman, and J. Q. Wu, Nano Lett. **13**, 2831 (2013).
[17] A. J. Hong, E. B. Song, H. S. Yu, M. J. Allen, J. Kim, J. D. Fowler, J. K. Wassei, Y. Park, Y. Wang, J. Zou, R. B. Kaner, B. H. Weiller, and K. L. Wang, ACS Nano **5**, 7812 (2011).
[18] P. Cui, S. Seo, J. Lee, L. Wang, E. Lee, M. Min, and H. Lee, ACS Nano **5**, 6826 (2011).
[19] G. H. Lee, Y. J. Yu, C. Lee, C. Dean, K. L. Shepard, P. Kim, and J. Hone, Appl. Phys. Lett. **99**, 243114 (2011).
[20] S. Bertolazzi, D. Krasnozhon, and A. Kis, ACS Nano **7**, 3246 (2013).
[21] Q. H. Wang, K. Kalantar-Zadeh, A. Kis, J. N. Coleman, and M. S. Strano, Nat. Nanotechnol. **7**, 699 (2012).
[22] M. Bernardi, M. Palummo, and J. C. Grossman, Nano Lett. **13**, 3664 (2013).
[23] W. J. Yu, Y. Liu, H. Zhou, A. Yin, Z. Li, Y. Huang, and X. Duan, Nat. Nanotechnol. **8**, 952 (2013).
[24] M. M. Furchi, A. Pospischil, F. Libisch, J. Burgdröfer, and T. Mueller, Nano Lett. **14**, 4785 (2014).
[25] Y. Z. Chen, B. Lee, D. N. Fu, and V. Podzorov, Adv. Mater. **23**, 5370 (2011).